

RI 9182

**RI 9182**

PLEASE DO NOT REMOVE FROM LIBRARY

**Bureau of Mines Report of Investigations/1988**

# **Strain Energy as a Basis for Optimizing Roof Truss Installations in Bedded Roof**

**By C. P. Mangelsdorf**



**UNITED STATES DEPARTMENT OF THE INTERIOR**



**Report of Investigations 9182**

# **Strain Energy as a Basis for Optimizing Roof Truss Installations in Bedded Roof**

**By C. P. Mangelsdorf**

**UNITED STATES DEPARTMENT OF THE INTERIOR  
Donald Paul Hodel, Secretary**

**BUREAU OF MINES  
T S Ary, Director**

Library of Congress Cataloging in Publication Data:

**Mangelsdorf, C. P.**

Strain energy as a basis for optimizing roof truss installations in bedded roof.

(Report of investigations/United States Department of the Interior, Bureau of Mines ; 9182)

Bibliography: p. 16

Supt. of Docs. no.: I 28.23:9182.

1. Mine roof control. 2. Roof trusses. I. Title. II. Series: Report of investigations (United States. Bureau of Mines) ; 9182.

TN23.U43

[TN288]

622 s [622'.28]

88-600082

## CONTENTS

	<u>Page</u>
Abstract.....	1
Introduction.....	2
Assumptions.....	3
Support available.....	3
Bending strain energy.....	4
Minimization of bending strain energy.....	6
Design examples--bending only.....	9
Shear strain energy.....	10
Minimization of total strain energy.....	12
Design examples--combined bending and shear.....	14
The influence of horizontal in situ stresses.....	14
Conclusions.....	15
References.....	16
Appendix A.--Bending strain energy.....	17
Appendix B.--Zero net displacement.....	19
Appendix C.--The effect of axial load on beam behavior.....	20
Appendix D.--Abbreviations and symbols used in this report.....	24

## ILLUSTRATIONS

1. Truss types.....	2
2. The geometry of one inclined chord.....	4
3. Shear and bending moment diagrams for roof beam.....	5
4. Bending strain energy contours.....	5
5. Optimum location for a bolt, $T = wL/2$ , $\ell = 0.2L$ .....	7
6. Optimum location for all bolts with $\beta/\lambda = 5.0$ .....	8
7. Optimum slope for angle bolts based on bending strain energy only.....	8
8. Shear strain energy contours.....	11
9. Optimum slope for angle bolts based on shear strain energy only.....	12
10. Effective region of conflict between optimum bending and optimum shear.....	13
11. Optimum slope for angle bolts based on bending and shear strain energies combined.....	13
C-1. Fixed-end beam-column relations.....	20
C-2. Fixed-end column relations.....	21

## TABLES

C-1. Comparison of amplification factors from equations C-6 and C-7.....	21
C-2. Comparison of amplification factors from equations C-29 and C-30.....	23

UNIT OF MEASURE ABBREVIATIONS USED IN THIS REPORT

ft	foot	lbf/ft <sup>3</sup>	pound (force) per cubic foot
in	inch	lbf/in <sup>2</sup>	pound (force) per square inch
kips/ft	kips per foot		
lb	pound	pct	percent
lbf/ft	pound (force) per foot		

# STRAIN ENERGY AS A BASIS FOR OPTIMIZING ROOF TRUSS INSTALLATIONS IN BEDDED ROOF

By C. P. Mangelsdorf<sup>1</sup>

---

## ABSTRACT

When the finely bedded shale frequently encountered over coal seams experiences a separation, the material below the separation must behave like a beam or plate in that it must resist both bending and shear. Because of the weakness in interlaminar shear inherent in such strata, shear deflections that are usually ignored in isotropic beam theory may account for a significant part of the total roof sag. Similarly, when a roof truss is installed in such a roof the upward displacement reducing the sag will have components due to shear as well as bending.

Questions asked by mine operators about the installation of roof trusses frequently deal with optimum position, slope, and initial tension of the inclined chords. This Bureau of Mines report examines the effects of those chord parameters on the strain energy of both shear and bending and offers optimum values that will minimize the total strain energy of the immediate roof.

Design charts are provided, several design examples are included, and the results are compared with current practice. The effects of in situ stresses are investigated and are shown to be equivalent to an additional load on the beam.

---

<sup>1</sup>Civil engineer, Pittsburgh Research Center, Bureau of Mines, Pittsburgh, PA, and faculty member, University of Pittsburgh.

## INTRODUCTION

In recent decades, the underground coal mining industry has seen the emergence of a device for main entry roof support called the roof truss. There are, at present, two basic types of trusses in common usage; the sling type and the angle-bolt type, both depicted in figure 1. Although different in some respects, they both rely on point anchorage over the ribs for their tensioned, inclined chords, and on a horizontal chord, or tie, which is also tensioned. The resultant force on the roof at each bearing plate or connecting bracket is more nearly vertical than it would be if there were not a tensioned horizontal chord.

In general, roof support requirements are difficult to define because one never knows, except empirically, how much support is enough. In the case of roof trusses, there are three factors affecting their performance, namely installation, stiffness, and strength. Considering only the first it would be useful to know:

1. Where to place the bearing plates or brackets.
2. At what angle to drill the holes for the inclined chords.
3. What tension to put into the inclined chords so as to achieve the most effective results for the effort and expense.

This paper examines the relevance of elementary beam mechanics to these questions for the case of a bedded roof. A minimum reliance on the roof properties will be used because they are seldom

known in sufficient detail and accuracy to permit meaningful calculations. Effectiveness will be measured by minimizing strain energy.

It is well known that a structural system in equilibrium with specified geometry, loads, and support conditions will deform in such a manner as to naturally minimize its strain energy. In attempting to optimize the support positions of a roof truss by further minimizing the strain energy of the roof beam, the investigators will be operating on the principle that the lower the strain energy, the more likely the beam can sustain its deformations without loss in structural integrity. In so doing, it must be assumed that stress levels at the most highly stressed points are sufficiently below failure so that failure at these points is not imminent.

The use of a beam concept in bedded roof is widely recognized but not highly regarded because of its apparent inability to explain some observed phenomenon even when bed separation is well defined. Part of this inability may be due to the common misconception that beams resist loads solely by bending. Although shear deformations in homogeneous beams are normally negligible, in the case of bedded roof, numerous bedding planes can provide planes of weakness in shear, the deformations across which can significantly increase a beam's deflection (1-2).<sup>2</sup> Therefore, shear strain energy as

<sup>2</sup>Underlined numbers in parentheses refer to items in the list of references preceding the appendixes.

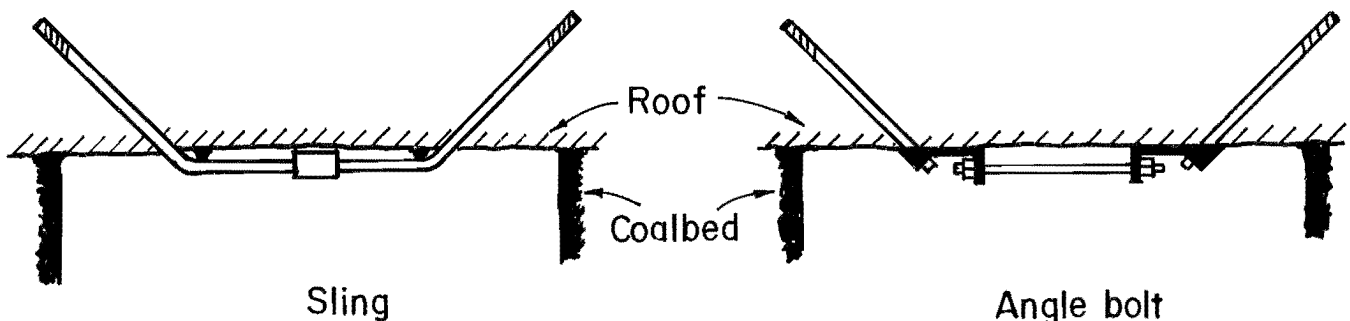


FIGURE 1.—Truss types.

well as bending strain energy will be incorporated in the calculations. The effects of axial stress due to in situ conditions will also be considered.

Two previous investigations have been made into the question of optimizing truss installation. The first in 1973 by Sheorey, Verma, and Singh (3) used only statics to examine the equilibrium at the bearing block of a sling-type truss. The goal was to optimize the support reactions without regard to the character or deformation of the roof. The authors apparently failed to recognize that the total uplift force on the roof is equal to the vertical component of the inclined chord tension. Through a series of assumptions, the authors arrived at the conclusion that the optimum conditions included a minimizing of the inclined chord tension.

Neall, Haycocks, Townsend, and Johnson (4-6) reported on photoelastic studies made on urethane rubber models of multiple-beam roofs supported by a miniature

truss. The models were allowed to deflect downward owing to simulated coal removal and were then pushed back up by a miniature sling-type truss. The tension in the truss was increased until either the anchorage failed, or the limit of truss adjustment was reached. Although many models were tested, the models for which the inclined chord slopes were 30°, 45°, and 60° from the horizontal were tested for only one roof span and only one truss span, and there was so much scatter in the data that no reasonable conclusion concerning optimum could be drawn.

In a parallel analytical study of a single elastic roof beam, the authors found that the optimum slope angle for reducing the tension at the bottom of the beam at midspan to zero was greater than 90°, the anchorage being above the entry opening rather than over the rib. It was a conclusion the authors were reluctant to endorse.

#### ASSUMPTIONS

This study will assume a uniform, but not homogeneous, immediate roof consisting of many layers of differing properties and experiencing at least one bed separation, so as to establish the existence of a beam. Except for possibly determining the horizon of the separation, the contribution of vertical bolts will be ignored. It is assumed that the separation takes place prior to the installation of the trusses. The stress-strain properties of the various layers may be quite different, but all must be approximately linear. They may even be time dependent, but it is assumed that this time dependence is the same for all

layers and does not vary with stress level. The beam is assumed to be completely fixed at its ends.

It is further assumed that the primary support provided by the truss is the vertical component of the inclined chord tension. Except for very shallow beams (depth-span ratios of 1/20 or less) and very small or very large horizontal chord tensions (compared with inclined chord tensions), this should be true. The results will be applicable to both angle-bolt and sling-type trusses. Because beam theory is being employed, the conclusions cannot necessarily be applied to intersections.

#### SUPPORT AVAILABLE

The geometry of one inclined chord is shown in figure 2. The length of the chord,  $l$ , not including the anchorage, is related to the location of the bearing plate,  $a$ , as measured from the rib, by the angle  $\theta$ , or

$$\theta = \cos^{-1} \left( \frac{a}{l} \right).$$

Although a safe anchorage zone can be described by a curved line tangent to the rib and arcing toward the center of the

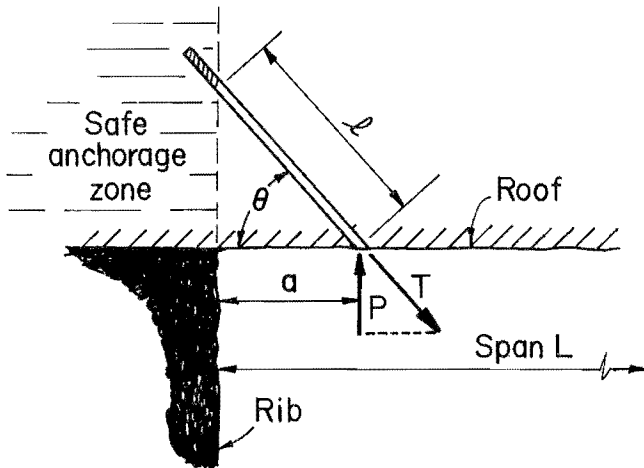


FIGURE 2.—Geometry of one inclined.

entry, it is conservative and convenient to assume a vertical line. The uplift,  $P$ , supplied by one chord is defined as

#### BENDING STRAIN ENERGY

The bending moment at any point in a beam fixed at both ends supporting a uniform load of  $w$  due to the beam's own weight and additionally supported by two symmetrically placed concentrated forces,  $P$ , as shown in figure 3, is given in two intervals. For  $0 < x < a$ , where  $x$  is measured from a fixed end,

$$M = -\frac{wL^2}{12} + \frac{wL}{2}x - \frac{wx^2}{2} + Pa \left(1 - \frac{a}{L}\right) - Px, \quad (3)$$

and for  $0 < x < (L/2) - a$ , where  $x$  is measured from center span,

$$M = \frac{wL^2}{24} - \frac{wx^2}{2} - \frac{Pa^2}{L}. \quad (4)$$

The bending strain energy for any beam is given by the expression (5, p. 173)

$$U_B = \int_0^L \frac{M^2 dx}{2EI}. \quad (5)$$

Substitution of equations 3 and 4 into 5 and the integration thereof, leads to a rather lengthy expression, which is given

$$P = T \sin \theta$$

$$\text{or } P = T \sin \left[ \cos^{-1} \left( \frac{a}{l} \right) \right] \quad (1)$$

where  $T$  is the chord tension.

It will be useful to put all of the calculations in terms of  $L$ , the overall span of the roof, and to define

$$\alpha = \frac{a}{L} \text{ and } \lambda = \frac{l}{L}$$

so that equation 1 becomes

$$P = T \sin \left[ \cos^{-1} \left( \frac{\alpha}{\lambda} \right) \right]. \quad (2)$$

in appendix A. It is this energy that an attempt is made to minimize. The quantity  $EI$  in equation 5 represents some effective value of bending stiffness that will remain unknown, but as long as it is constant over the length of the beam it does not have to be known. In a similar way the load,  $w$ , in equations 3 and 4 can remain unknown, although if the horizon of the first bed separation is known,  $w$  can be estimated, as will be necessary for specific numerical examples.

Thus, the bending strain energy becomes a function of two variables  $P$  and  $a$ . It will be convenient to express  $P$  in terms of  $w$  by the ratio

$$\eta = \frac{P}{wL/2}, \quad (6)$$

and, as in the previous section,  $a$  can be represented by the ratio  $\alpha = a/L$ . With these substitutions the bending strain energy surface can be plotted for the beam in terms of the coordinates  $\eta$  and  $\alpha$ . Figure 4 is such a plot showing contours of equal energy for the left half of the beam.

There are several features of figure 4 that must be noted. First, the absolute minimum energy occurs when  $\alpha = 0.33$  (or when the overall span  $L$  is divided into three equal spans of  $L/3$  each) and when

$\eta = 0.67$  (or when  $P = wL/3$ , which also happens to be twice the magnitude of the rib shears for this case). Although this point would appear to be a partial solution of the problem there are practical difficulties that could prevent its being achieved. If the angle bolts are used as part of the bolting plan, the one-third points may not be appropriate. It could also be that it is impossible to drill two holes simultaneously with dual drill booms located at the one-third points and tilted to the angle eventually found to be optimum. Or if drillable, such holes might be too long, taking too much time to drill and requiring too long an inclined chord. Also, enough uplift may not be achieved to reach optimum conditions. For these reasons it will be useful to contemplate other points on the strain energy surface.

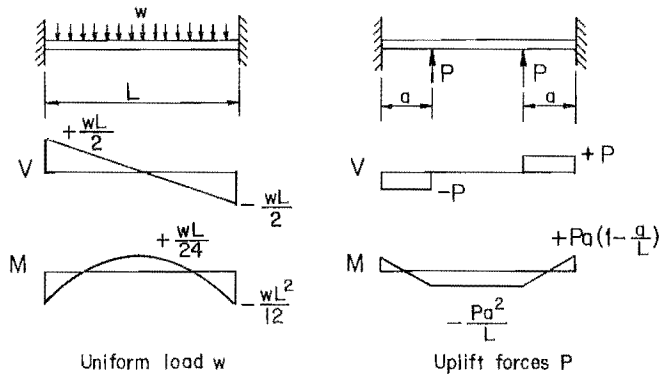


FIGURE 3.—Shear and bending moment diagrams for roof beam.

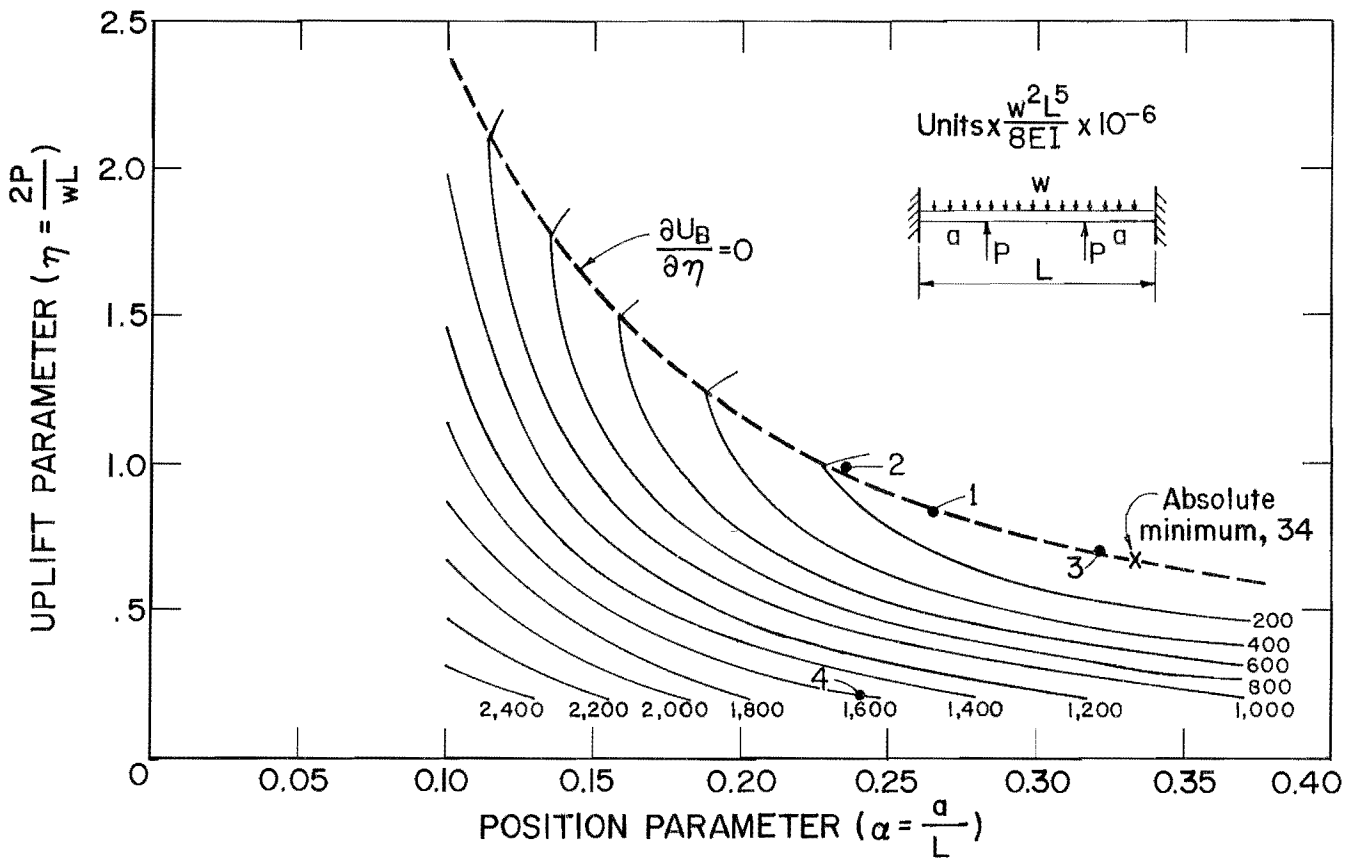


FIGURE 4.—Bending strain energy contours. Numbered dots correspond to numbered examples in text.

The second item of note in figure 4 is that not all of the contours have been drawn for the entire half of the beam. Values of  $\alpha$  less than 0.1 or greater than 0.35 are, of course, possible but are generally not practical, and their absence will not affect the conclusions. Values of  $\eta$  less than 0.2 are quite possible but again, they are not necessary for this discussion.

Finally, the dashed line labeled " $\partial U_B/\partial \eta = 0$ " passing through the minimum

point in figure 4 (the "valley" in the strain energy surface) corresponds to values of  $\eta$  and  $\alpha$  for which the net vertical displacements at the intermediate support points are zero. This represents a practical upper limit on  $\eta$  because the forces  $P$  can never, for practical purposes, push the beam up farther than it had come down, no matter how large  $P$  is. For this reason energy contours for  $\eta$  values above  $\partial U_B/\partial \eta = 0$  have not been completed.

#### MINIMIZATION OF BENDING STRAIN ENERGY

To appreciate how the variation of angle-bolt geometries interacts with the strain energy surface of figure 4, it is necessary to express equation 2 for the uplift force available in the same units as figure 4. To do this, both sides of equation 2 are divided by the quantity  $wL/2$ , and the notation  $\beta = 2T/wL$  is introduced so that equation 2 becomes

$$\eta = \beta \sin \left[ \cos^{-1} \left( \frac{\alpha}{\lambda} \right) \right]. \quad (7)$$

Thus for any angle bolt tension,  $\beta$ , and length of bolt,  $\lambda$ , the uplift  $\eta$  is a function of  $\alpha$ . On a plot such as figure 4, equation 7 will appear as a quarter of an ellipse with its center at  $\alpha = \eta = 0$ , its vertical intercept at  $\alpha = 0$ ,  $\eta = \beta$  and its horizontal intercept at  $\eta = 0$ ,  $\alpha = \lambda$ . In terms of truss geometry, the vertical intercept corresponds to a bolt that is vertical and, therefore, all of the tension goes into uplift, but for which the bracket is at the rib doing nothing to reduce strain energy in the beam. The horizontal intercept, on the other hand, corresponds to a bolt that is horizontal. The bracket is as far away from the rib as possible but there is no uplift. It is along the arc between these two extremes that the optimum solution lies.

To illustrate this concept consider an angle bolt for which  $\beta = 1.0$  ( $T = wL/2$ ) and  $\lambda = 0.2$  ( $l = 0.2L$ ). The ellipse for this bolt is shown in figure 5, superimposed on the strain energy contours of figure 4. The optimum geometry of the bolt can be found by following the curve

of the bolt until a tangent to the ellipse is parallel to a tangent to a strain energy contour at the same point. Such a point is labeled "A" in figure 5, with approximate coordinates of  $\eta = 0.6$  ( $P = 0.3 wL$ ) and  $\alpha = 0.16$  ( $a = 0.16L$ ). Moving along the ellipse in either direction from point A would be moving to higher strain energy levels. The optimum slope angle,  $\theta$ , for point A can be found from the expression

$$\theta = \cos^{-1} \left( \frac{\alpha}{\lambda} \right), \quad (8)$$

which for this case is approximately  $38^\circ$ . If figure 5 had been drawn to a combination of scales for  $\alpha$  and  $\eta$  such that the ellipse appeared as a circle the slope of the line OA would actually be  $38^\circ$ .

One of the very interesting characteristics of plots such as figure 5 is that ellipses of the same aspect ratio appear to have the same optimum slope. Figure 6 shows a family of ellipses with an aspect ratio ( $\beta/\lambda$ ) of five. All of the optima (except for the largest ellipse shown, which will be discussed below) lie along the same radial line OB through the origin. Whether this relationship is exactly valid or only approximately so could be determined by mathematical analysis but is sufficiently valid for present purposes in that a small error in the location of point A, for example, does not lead to a significantly different value of strain energy.

Plots similar to figure 6 have been drawn for different aspect ratios and the results plotted on log-log paper. The

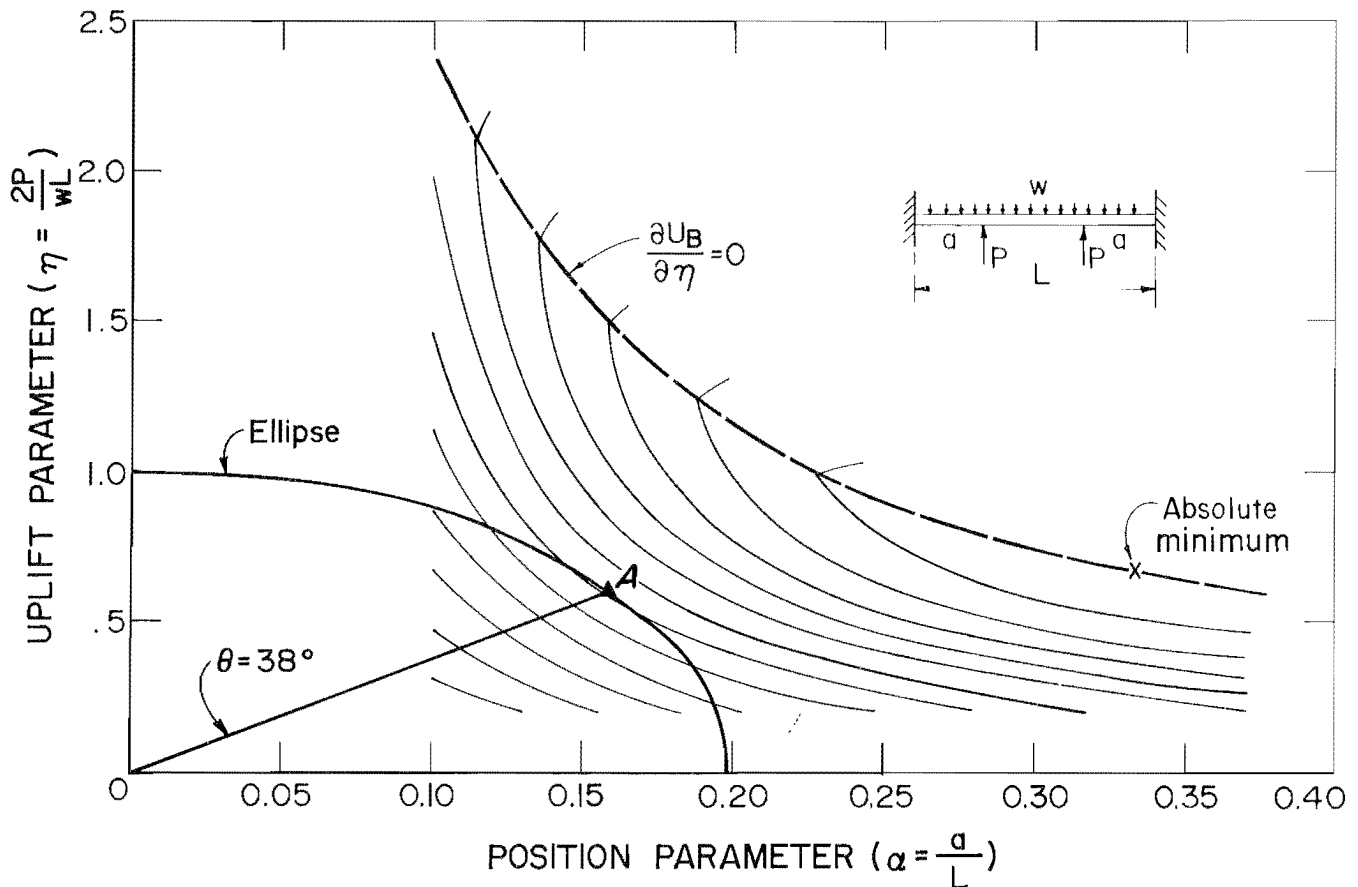


FIGURE 5.—Optimum location for a bolt,  $\tau = wL/2$ ,  $\nu = 0.2L$ .

end product is a reasonably straight line for the optimum ratio  $\eta/\alpha$  given by the equation

$$\frac{\eta}{\alpha} = 0.96 \left( \frac{\beta}{\lambda} \right)^{0.84} \quad (9)$$

If equation 7 is written in the more common form for an ellipse it becomes

$$\frac{\alpha^2}{\lambda^2} + \frac{\eta^2}{\beta^2} = 1, \quad (10)$$

from which  $\alpha$  can be expressed as

$$\alpha = \beta \sqrt{\frac{1}{\frac{\beta^2}{\lambda^2} + \frac{\eta^2}{\alpha^2}}} \quad (11)$$

Substituting equation 9 squared into equation 11 and dividing both sides by  $\lambda$  results in

$$\frac{\alpha}{\lambda} = \frac{\beta}{\lambda} \sqrt{\frac{1}{\frac{\beta^2}{\lambda^2} + 0.924 \left( \frac{\beta}{\lambda} \right)^{1.68}}} \quad (12)$$

from which the optimum ratio  $\alpha/\lambda$  can be found for any aspect ratio. Knowing the ratio  $\alpha/\lambda$ , the optimum slope  $\theta$  can be determined from equation 8. The solution of equation 8 into which equation 12 has been substituted is shown in figure 7 for a reasonable range of aspect ratios.

Before the use of figure 7 is demonstrated for design purposes, however, it is necessary to consider one limitation

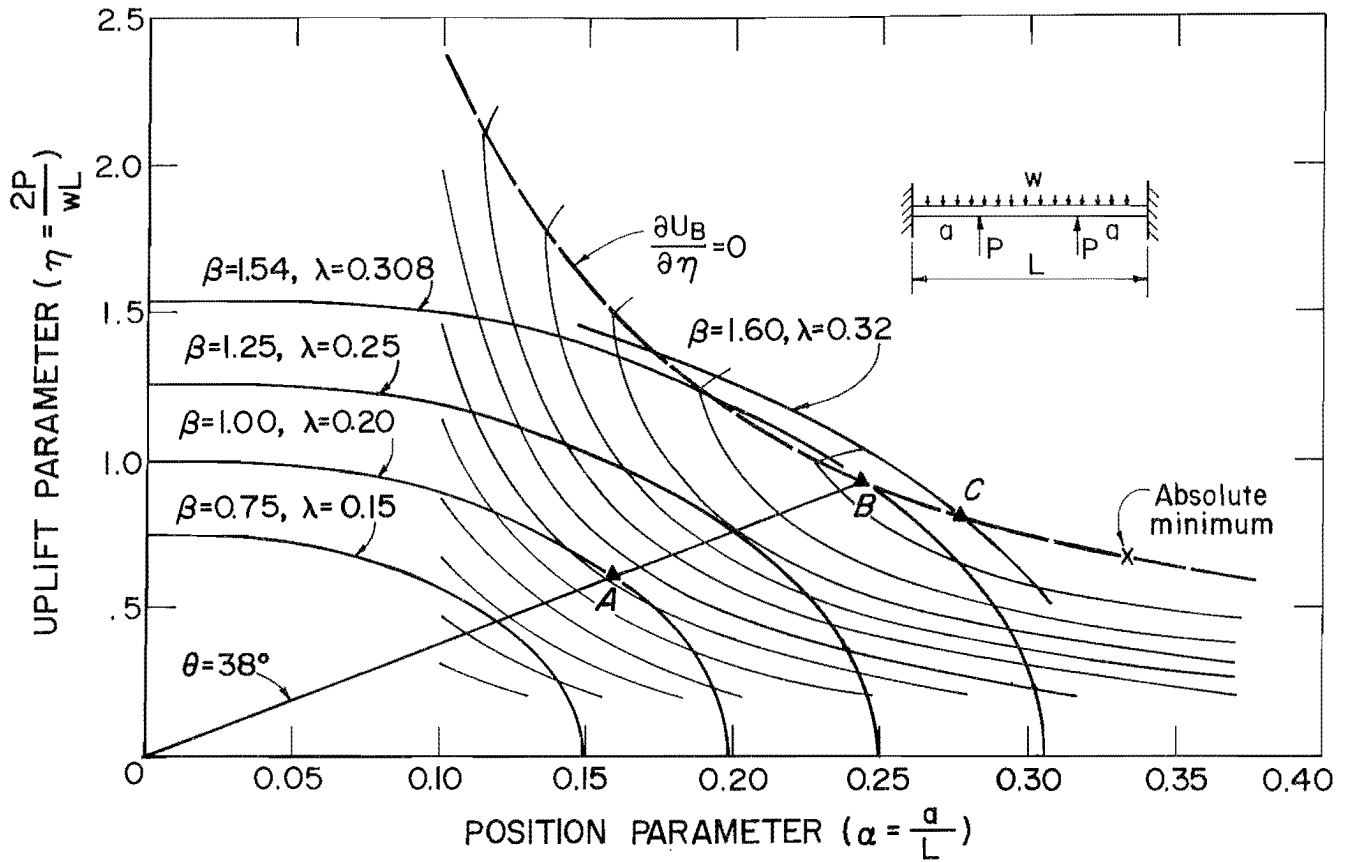


FIGURE 6.—Optimum location for all bolts with  $\beta/\lambda = 5.0$ .

to the data presented there. For an ellipse larger than the one that intersects  $\partial U_B/\partial \eta = 0$  at point B in figure 6, the relationships in figure 7 are no longer valid. The optimum for such a case is the lower intersection of the ellipse with the  $\partial U_B/\partial \eta = 0$  line, as for example, point C in figure 6. When this occurs, the optimum coordinates must be found from plotting the ellipse on the strain energy contours as in figures 5 and 6 or by simultaneously solving the equations for the ellipse and  $\partial U_B/\partial \eta = 0$  as given in appendix A. For convenience, the maximum value of  $\alpha$  for which figure 7 is valid is also given in figure 7.

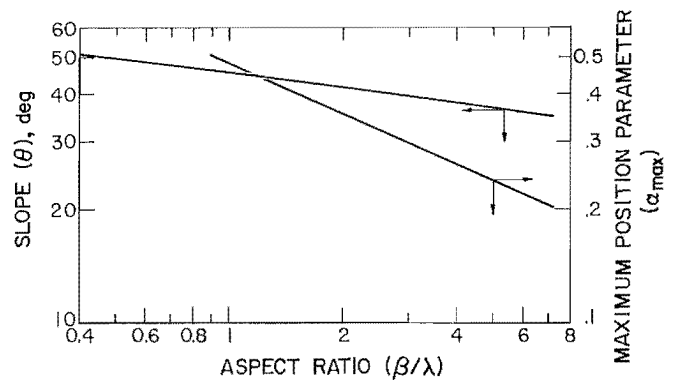


FIGURE 7.—Optimum slope for angle bolts based on bending strain energy only.

DESIGN EXAMPLES<sup>3</sup>--BENDING ONLY

1. Suppose a truss installation is being considered for the roof of an 18-ft entry in which a bed separation occurs 2 ft above the roof line. Six-foot-long angle bolts (exclusive of anchorage over the rib) at 4-ft centers are contemplated at a tension of 15,000 lb. For these conditions and assuming the roof material weights 150 lbf/ft<sup>3</sup>, it is noted that

$$L = 18 \text{ ft,}$$

$$T = 15,000 \text{ lb,}$$

$$h = 2 \text{ ft,}$$

$$\ell = 6 \text{ ft,}$$

$$w = 2 \times 4 \times 150 = 1,200 \text{ lbf/ft,}$$

$$wL/2 = \frac{1,200 \times 18}{2} = 10,800 \text{ lb,}$$

$$\beta = T/(wL/2) = \frac{15,000}{10,800} = 1.39,$$

$$\lambda = \ell/L = \frac{6}{18} = 0.333,$$

$$\text{and } \beta/\lambda = \frac{1.39}{0.333} = 4.17.$$

From figure 7, it is found that

$$\theta = 37^\circ, \quad \alpha_{\max} = 0.269,$$

$$\alpha = 0.333 \cos 37^\circ = 0.266$$

$$< 0.269,$$

$$\eta = \beta \sin \theta = 0.836,$$

$$\text{and } a = 0.266 \times 18 = 4.79 \text{ ft.}$$

Mark the roof for drilling about 4 ft 9 in from the rib and drill at 37° from the horizontal. This example is represented by point 1 on figure 4.

2. Because low angles of drilling result in more bit "walking" toward the rib producing bending in the drill steel, suppose the drill operator is instructed to drill at 45° with a corresponding decrease in the support position,  $a$ , to maintain the same bolt length. What are the consequences? From equation 8,

$$\frac{\alpha}{\lambda} = \frac{a}{\ell} = \cos \theta = 0.707,$$

$$\alpha = \lambda \cos \theta,$$

$$\text{and } 0.333 \times 0.707 = 0.235.$$

From equation 7,

$$\eta = \beta \sin 45^\circ$$

$$\text{and } 1.39 \times 0.707 = 0.982.$$

Plotting  $\alpha$  and  $\eta$  for this case (example 2) on figure 4 and comparing it with the coordinates of the first example, it is seen that the strain energy for this case is approximately twice as great, although it is still more than an order of magnitude less than it would have been without the truss. An optimum design in this example has not been achieved because the solution has been over constrained. By specifying three of the four variables in the equation for the ellipse, equations 7 or 10, the fourth variable is determined independently of energy considerations.

3. Suppose the separation in the first example occurs at 1 ft instead of 2 ft.  $\beta/\lambda$  doubles to become 8.34. Extrapolating from figure 7, it is found that

$$\theta = 34^\circ, \quad \alpha_{\max} = 0.202,$$

<sup>3</sup>In the design examples, "USE" identifies that the calculations have achieved a workable solution; "N.G." (no good) identifies the contrary.

and  $\alpha = 0.333 \cos 34^\circ = 0.276$   
 $> 0.202$  N.G.

Figure 7 does not apply.

Graphically solving equations 10 and A-9 simultaneously leads to the optimum coordinates  $\alpha = 0.322$  and  $\eta = 0.70$ , from which it is found that  $a = 5.80$  ft and  $\theta = 15^\circ$ , a thoroughly impractical solution. As can be seen after a little reflection, solutions for which figure 7 does not apply will always be for drilling angles less than those for which it does apply. Since much of figure 7 corresponds to drilling angles less than  $45^\circ$ , there is no practical reason to use solutions not covered by figure 7.

4. The figures used in the previous examples were intended to help in the understanding of the influence of the various parameters and the limitations of the graphs. Now suppose a more realistic case in which the vertical bolts of example 1 are 6 ft long, so that they cause a beam 6 ft deep to develop. If  $T$  is taken as 10,000 lb and the length and spacing of angle bolts remains the same,

$$\beta = \frac{10,000}{3 \times 10,800} = 0.31,$$

which leads to

$$\frac{\beta}{\lambda} = \frac{0.31}{0.33} = 0.93.$$

From figure 7, it is found that

$$\theta = 44^\circ, \quad \alpha_{\max} = 0.50,$$

$$\alpha = 0.33 \cos 44^\circ = 0.24 < 0.50,$$

and  $a = 0.24 \times 18 = 4.3$  ft

USE 4 ft 3 in.

This solution is labeled as 4 in figure 4 and is not much different from standard practice. Increasing  $T$  or lengthening the angle bolt will obviously improve the situation. Ideal conditions for this roof would be for  $\alpha = 0.33$  with  $T = 33,800$  lb,  $l = 7.8$  ft, and  $\theta = 39.7^\circ$ . The strain energy level for ideal conditions is about 2 pct of that for the above solution.

#### SHEAR STRAIN ENERGY

The procedure for dealing with shear strain energy is identical to that for bending. It may be useful, however, to consider first some necessary assumptions that are unique to shear. The first of these is that in the beam, a multitude of thin, inter-bed layers exist whose shear moduli are several orders of magnitude lower than that of the bedding material. It is further assumed that the deformations across these layers are proportional to the shear stresses predicted for a homogeneous beam of the same depth and that the cumulative effect of these deformations is to produce a deflected shape of the beam due to shear alone in which the slope is proportional to the shear diagram for the beam. With these conditions, the shear deflections can be of the same order of magnitude as the

bending deflections, as would occur in a homogeneous beam whose shear modulus is much lower than that required by elasticity theory. Although there is no direct evidence to prove the existence of large deformations within these thin, inter-bed layers, there is evidence of roof beam deflections significantly in excess of what would be predicted from the bending strain on the bottom surface or from the normal stress-strain relations for the bedding material (1).

It is equally easy and probably more reasonable to visualize shear deformations in bedded beams as finite slip between relatively rigid bedding planes in the regions of the beam with the highest shear load. The deflected shape and, hence, the strain energy of the beam due to shear would not differ much from

that predicted by the above assumptions, however. As will be shown below, the exact distribution of the strain energy due to shear and for that matter, the distinctions between bending and shear deformations will begin to blur as the study proceeds.

As in bending, the shear diagrams in figure 3 are given in two intervals. For the interval  $0 \leq x \leq a$ ,

$$V = \frac{wL}{2} - wx - P = \frac{wL}{2} \left(1 - \frac{2x}{L} - \eta\right), \quad (13)$$

and for the interval  $0 \leq x \leq (L/2) - a$ , where  $x$  is measured from center span

$$V = wx. \quad (14)$$

The shear strain energy is given (5, p. 173) by

$$U_s = \int_0^L \frac{v^2 dx}{2AG}, \quad (15)$$

in which the quantity  $AG$ , like  $EI$  in bending, is some effective value that will remain unknown.

Substitution of equations 13 and 14 into equation 15 and the result of integration is contained in appendix A. The strain energy contours for shear are plotted in figure 8. As in the case of bending, there is a "valley" corresponding to zero shear deflections or  $\partial U_s / \partial \eta = 0$ . The absolute minimum for this plot is also at  $\eta = 0.67$ ,  $\alpha = 0.33$ . Contours over the same range as figure 4 have been included because it is possible with two kinds of deflections that values of  $\eta$  above the  $\partial U_s / \partial \eta = 0$  line for shear could exist. That is, for a certain range of values of  $P$ , shear deflections upward due to  $P$  might be greater than the downward shear deflections due to  $w$ , but the bending deflections could still be downward to the extent that the net deflections could be downward or zero.

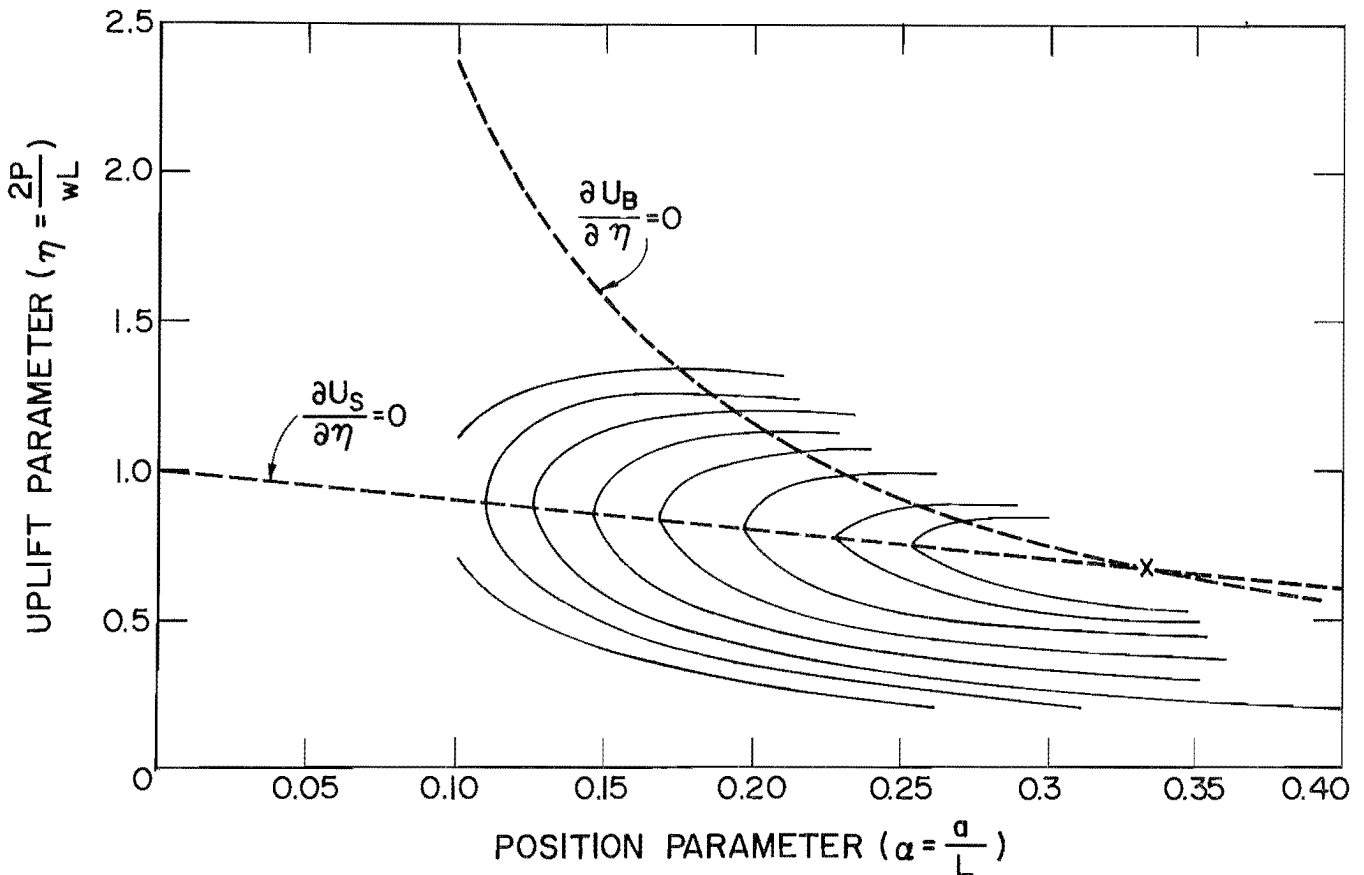


FIGURE 8.—Shear strain energy contours.

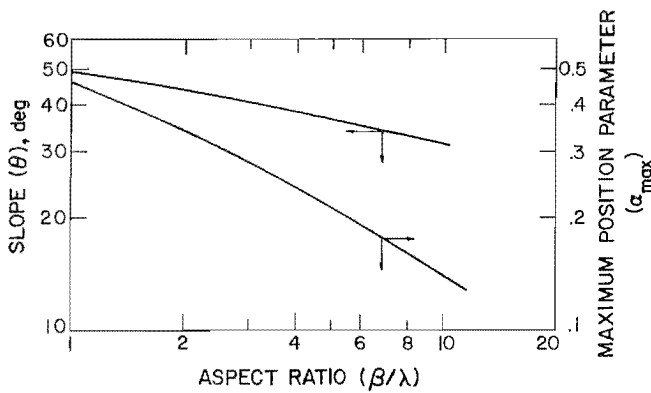


FIGURE 9.—Optimum slope for angle bolts based on shear strain energy only.

#### MINIMIZATION OF TOTAL STRAIN ENERGY

It should now be possible, in theory at least, to combine the two strain energy expressions in equations 5 and 15 and find optimum conditions for any case. The practical difficulty with this idea is that it requires a knowledge of the relative magnitudes of  $EI$  and  $AG$ , quantities unknown from the outset. Thus, meaningful but approximate conclusions must be reached from the information known.

Perhaps the most useful conclusion and the easiest to reach applies to the range of values of  $\eta$  and  $\alpha$  that fall below the  $\partial U_S/\partial \eta = 0$  line in figure 8. In this range the strain energy contours for shear and bending are quite similar. Thus, some kind of average of equations 9 and 16 leads to fairly small errors in both the bending and shear strain energy minima because the angle-bolt ellipses do not diverge rapidly from the strain energy contours in this region.

For values of  $\eta$  and  $\alpha$  that lie between the curves  $\partial U_S/\partial \eta = 0$  and  $\partial U_B/\partial \eta = 0$  in figure 8, no such approximation is possible. In this region the part of the angle-bolt ellipse that is near optimum for bending is almost perpendicular to the strain energy contours for shear. The minimum condition for shear alone ought to be along the  $\partial U_S/\partial \eta = 0$  curve of figure 8.

However, there are two considerations that reduce the effective size of this conflicting region. The first is based on the observation, previously noted,

Plotting of ellipses as before leads to the approximate relation

$$\eta/\alpha = 1.17(\beta/\lambda)^{0.72}. \quad (16)$$

from which is found

$$\frac{\alpha}{\lambda} = \frac{\beta}{\lambda} \sqrt{\frac{1}{\frac{\beta^2}{\lambda^2} + 1.37 \left(\frac{\beta}{\lambda}\right)^{1.44}}}. \quad (17)$$

Calculations for optimum  $\theta$  and  $\alpha_{max}$  also follow directly from equation 16 and are plotted in figure 9, similar to figure 7.

that deflections upward due to truss installation might involve more shear component than was present in the original downward movement due to gravity. This must be true for points above the  $\partial U_S/\partial \eta = 0$  curve of figure 8. Thus, it will be impossible in the presence of significant shear deformations to reach points along the line  $\partial U_B/\partial \eta = 0$  during installation. Using specific values of  $G$  relative to  $E$  and  $h$  relative to  $L$ , lines corresponding to zero net displacement in the presence of both shear and bending deformation have been worked out in appendix B and are plotted in figure 10. These are intended for rough guidance only, as they are based on uniform properties of the layers.

The other consideration that reduces the effective size of the conflicting region is a practical one. If it is admitted that holes at angles less than  $35^\circ$  from the horizontal will probably not be drilled, the value of  $\alpha/\lambda$  is limited to a maximum value of 0.819. From equations 12 and 17, it is seen that this leads to maximum values of  $\beta/\lambda$  of about 7 and 6, for bending and shear, respectively. These limits are also shown in figure 10. The now reduced region where optimum positions for shear and bending are in conflict is indicated by the cross-hatching. This area is sufficiently small and at an energy level so low that the limitations determined by averaging in some fashion the curves of

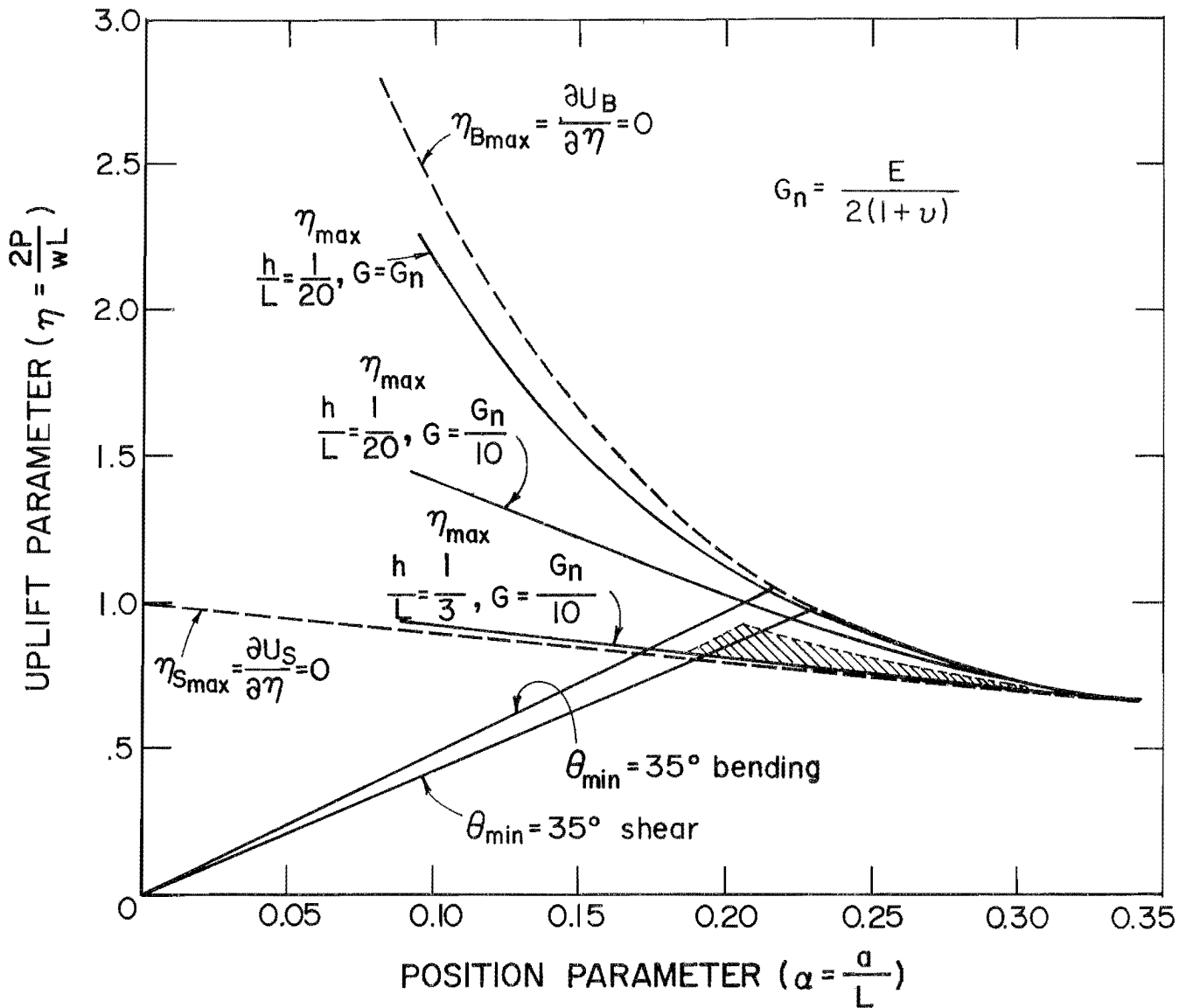


FIGURE 10.—Effective region of conflict between optimum bending and optimum shear.

figure 7 and 9 will not be significantly in error for points within this area.

In averaging, it is important to recognize that although bending strain energy can occur in the absence of significant shear strain energy, the reverse is generally not true. In fact, shear energy equal to bending energy probably represents a reasonable upper limit of significant shear participation. Thus, an average weighted toward bending in the approximate ratio 2:1 is reasonable. This has been done by averaging equations 9 and 16. The result is shown in figure 11 where the average curve for  $\theta$  for various  $\beta/\lambda$  has been plotted. An

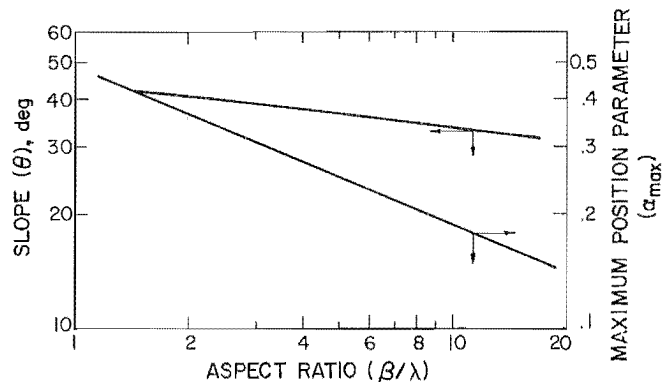


FIGURE 11.—Optimum slope for angle bolts based on bending and shear strain energies combined.

estimated  $\alpha_{max}$  curve based upon the two  $\partial U/\partial \eta = 0$  curves has also been included. The new working curves have the equations

$$\theta = 45.5(\beta/\lambda)^{-0.13} \quad (18)$$

and

$$\alpha_{max} = 0.48(\beta/\lambda)^{-0.44}. \quad (19)$$

$\alpha_{max}$  has a theoretical limit of 0.33.

#### DESIGN EXAMPLES--COMBINED BENDING AND SHEAR

5. Using the data of example 4 (for which  $\beta/\lambda$  was 0.93), it is found from figure 11 by extrapolation that

$$\begin{aligned} \theta &= 46, & \alpha_{max} &= 0.49, \\ \alpha &= \lambda \cos 46^\circ = 0.33 \cos 46^\circ \\ &= 0.23 < 0.49, \end{aligned}$$

and

$$a = \alpha L = 0.23 \times 18 \text{ ft} = 4.16$$

USE 4 ft 2 in.

6. Suppose experience shows that a second separation will occur 8 ft above the roof line. Assuming the same unit weight for this additional material,  $w$  will increase by a factor of 1.33, thereby reducing  $\beta$  and  $\beta/\lambda$  by the same factor, since the other parameters,  $T$ ,  $\ell$ , and  $L$  remain unchanged.  $\beta/\lambda$  becomes 0.70 and the design proceeds as before.

It would appear that the beam is not 8 ft deep, but is 6 ft deep with a superimposed load. However, the calculations proceed as though the beam were 8 ft deep. The upper beam will be partially self-supporting. It therefore contributes strain energy as well as weight.

Proceeding with the design example, it is found from figure 11 for  $\beta/\lambda = 0.7$  that

#### THE INFLUENCE OF HORIZONTAL IN SITU STRESSES

The effect of horizontal in situ stresses on roof beam behavior is to increase the vertical deflections already present due to gravity loading. This amplification effect is due to the horizontal forces at the ends of the beam interacting with the initial displacements to produce additional moments and shears that in turn produce additional displacements. Thus, the beam deflects as though it has more weight than its depth would suggest.

$$\theta = 47.8^\circ \text{ USE } 48^\circ$$

and

$$\alpha = 0.33 \cos 48^\circ = 0.22.$$

This is essentially the same design as in example 5. It demonstrates, as does figure 11, how insensitive  $\theta$  is to  $\beta/\lambda$ . This insensitivity helps to explain the relative success of installing trusses with virtually the same geometry in a wide variety of mines.

7. A common practice is to install at  $\theta = 45^\circ$  and  $\alpha = 0.2$ . What optimum tension might be recommended for such a truss to help support the roof of example 4? From figure 11,

$$\beta/\lambda = 1.07 \text{ and } \alpha_{max} > 0.2.$$

In this case,  $\lambda = \alpha \sqrt{2} = 0.28$ ,

$$\text{and } \beta = 1.07 \times 0.28 = 0.30,$$

therefore

$$\begin{aligned} T &= (wL/2) \cdot \beta = 32,400 \times 0.30 \\ &= 9,800 \text{ lb.} \end{aligned}$$

Again, if a greater tension is possible it makes sense to use it, although one can always do even better by changing  $\theta$  as well.

As shown in appendix C, the amplification factor for displacements can be conveniently and conservatively approximated by the expression

$$A.F. = \frac{1}{1 - Q/Q_c} \quad (20)$$

in which  $Q$  is the resultant axial force on the beam and  $Q_c$  is the value of  $Q$  that could produce elastic buckling in the

beam without truss support even in the absence of any gravity loading. When significant shear deflections are possible,  $Q_c$  is defined by

$$Q_c = \frac{\frac{4\pi^2 EI}{L^2}}{1 + \frac{4\pi^2 EI}{L^2 AG}} \quad (21)$$

For values of  $Q/Q_c$  less than 0.5 the amplification factor, as represented by equation 20, is, at worst, only 10 pct too high (compared with a more exact analysis, appendix C) for a beam subjected only to its own weight. Therefore, the calculated weight,  $w$ , can be multiplied by the amplification factor in equation 20 to obtain an effective value of the weight for use in determining optimum conditions in the previous section.

It will be noted, however, that to evaluate equation 21 and then 20 numerical values must be known not only for the in situ stress but also for both  $EI$  and  $AG$ , quantities previously avoided because

of their uncertainty. However, a rough estimate can give an idea of the significance of this effect.

Assume, for example, a worst case condition of a horizontal stress of 1,000 lbf/in<sup>2</sup> in excess of what would be predicted from the depth of overburden. Assume also that a beam of 12 in depth has formed over an entry 20 ft wide. From this information,  $Q$  is found to be 144 kips/ft width of beam. If an average value of  $E = 1 \times 10^6$  lbf/in<sup>2</sup> (perhaps given by a compression test normal to the bedding planes) and  $G = 38,000$  lbf/in<sup>2</sup> (about one-tenth of what it would be for a homogeneous material) is used,  $Q_c$  can be estimated from equation 21 to be 9.75 kips. From equation 20 the amplification factor becomes 1.2. If the estimate of material properties was high by a factor of two, the amplification factor would be low by only 14 pct. For deeper beams or shorter spans the error would be less. Thus, in the case of horizontal stress effects, estimation may overcome the lack of information.

## CONCLUSIONS

By minimizing strain energy, it is possible to optimize inclined chord location and tensions for roof truss installations. Furthermore, the criteria for minimizing shear and bending strain energies separately are found to be, for the most part, mutually inclusive so that a single curve can be used to optimize chord parameters. Except in the case of compressive horizontal in situ stresses, a knowledge of the relative roof properties in bending and shear are not required. The method allows for evaluating suboptimum conditions.

The results, however, are dependent upon many assumptions that may not be true. For example, the assumption of complete beam end fixity is valid only when the stiffness of the material above and below the beam is much, much greater than for the beam itself. The effect of less than complete fixity deserves to be studied. For another example, the

linearly elastic bending and shear deformation models employed are not likely to be encountered in the field. As noted earlier, the shear deformation model is particularly oversimplified and could be replaced by a more realistic behavior.

While the strain energy approach has at least a rational basis for beams in which no cross section is near impending failure, there is a school of thought that holds that the safest design is that for which the maximum shear and moment are least. Although optimum conditions for minimizing the maximum shear and moment may be mutually exclusive, it would be worth knowing how far off their optima a minimum energy solution would lie.

There are, naturally, many questions to be answered and many refinements that could be introduced. It is sufficient to note in conclusion that until something better comes along, the concept appears to provide a practical means of

estimating the required conditions for optimizing roof truss installations when bed separations are present.

Furthermore, the method tends to substantiate successful results in practice.

#### REFERENCES

1. Radcliffe, D. E., and R. M. Stateham. Long-Term Response of a Coal Mine Roof to Time Lapse Between Exposure and Support. BuMines TPR 110, 1980, 12 pp.
2. Mangelsdorf, C. P. Design of a Roof Truss Bolting Plan for Bear Mine. Paper in Proceedings of Fourth Conference on Ground Control, West Virginia Univ., Morgantown, WV, 1985, pp. 11-17.
3. Sheorey, R. R., B. P. Verma, and B. Singh. An Analysis of the Roof Truss. J. Mines, Met. and Fuels (Calcutta, India) v. 21, No. 8, Aug. 1973, pp. 233-236.
4. Neall, G. M., C. Haycocks, J. M. Townsend, and L. P. Johnson. Design Optimization in Underground Coal Systems - Volume VIII - The Roof Truss: An Analysis with Applications to Mine Design. Final Report, contract No. US DOE DE-AC01-76-ET-10722, VA Polytech. Inst. 2nd State Univ., Blacksburg, VA, 1981, 341 pp.
5. Neall, G. M., C. Haycocks, J. M. Townsend, and L. P. Johnson. Influence of Some Critical Design Parameters on Roof Truss Support Capacity - A Preliminary Report. Paper in Rock Mechanics Applications in Mining (Proc. 17th Symp. on Rock Mech., Snowbird, UT, 1976). Soc. Min. Eng. AIME, 1977, pp. 228-233.
6. \_\_\_\_\_. Optimizing Truss Installations With Body-Loaded Photoelastic Models. Trans. Soc. Min. Eng. AIME, v. 30, No. 6, June 1978, 660-666.
7. Laursen, H. I. Structural Analysis. McGraw-Hill, 1969, pp. 201-206.

## APPENDIX A.--BENDING STRAIN ENERGY

The total bending strain energy for a beam is given by the expression

$$U_B = \int_0^L \frac{M^2 dx}{2EI}, \quad (A-1)$$

where  $M$  is the bending moment, which is a function of  $x$ . For the loading in figure 3 and for the interval  $0 \leq x \leq a$  ( $x$  measured from the fixed end),

$$M = -\frac{wL^2}{12} + \frac{wL}{2}x - \frac{w}{2}x^2 + Pa \left(1 - \frac{a}{L}\right) - Px. \quad (A-2)$$

For the interval  $0 \leq x \leq (L/2) - a$  ( $x$  measured from midspan)

$$M = \frac{wL^2}{24} - \frac{w}{2}x^2 - \frac{Pa^2}{L}. \quad (A-3)$$

Using the substitutions

$\eta = \frac{P}{wL/2}$  and  $\alpha = a/L$  in equations A-2 and A-3 leads to

$$M = \frac{wL^2}{2} \left[ -\frac{1}{6} + \eta\alpha(1 - \alpha) + (1 - \eta) \frac{x}{L} - \frac{x^2}{L^2} \right] \quad (A-4)$$

and

$$M = \frac{wL^2}{2} \left( \frac{1}{12} - \eta\alpha^2 - \frac{x^2}{L^2} \right). \quad (A-5)$$

Squaring both equations A-4 and A-5, integrating over their appropriate intervals and adding the results yields

$$U_B = \frac{w^2L^5}{8EI} \left( A^2\alpha + AB\alpha^2 + \frac{B^2 - 2A}{3}\alpha^3 - \frac{B}{2}\alpha^4 + \frac{\alpha^5}{5} + \mu D^2 - \frac{2\mu^3}{3}D + \frac{\mu^5}{5} \right), \quad (A-6)$$

in which

$$A = \eta\alpha(1 - \alpha) - \frac{1}{6},$$

$$B = 1 - \eta,$$

$$D = \frac{1}{12} - \eta\alpha^2,$$

and

$$\mu = \frac{1}{2} - \alpha.$$

Equation A-6 is for one-half of the beam only. It is contours of the quantity within the parentheses of equation A-6 that appear in figure 4.

The displacement of the beam at the location of the uplift force  $P$  can be found from Castigliano's Second Theorem (7),<sup>1</sup> which states that

$$\Delta_P = \frac{\partial U_B}{\partial P}. \quad (\text{A-7})$$

To find the value of  $P$  when  $\Delta_P = 0$  it is easier to operate according to equation A-7 on equation A-1 and then integrate than to integrate equation A-6 squared and then operate:

$$\frac{\partial U_B}{\partial P} = 0 = \int_0^L \frac{M}{EI} \frac{\partial M}{\partial P} dx \quad (\text{A-8})$$

Finding the derivative of  $M$ , multiplying by  $M$  and integrating over the appropriate interval for equations A-2 and A-3 independently and adding the results yields

$$\eta = \frac{\alpha + \frac{1}{\alpha} - 2}{6 \left( \frac{2}{3} - \alpha \right)}, \quad (\text{A-9})$$

which is the equation of the "valley" in figure 4.

#### SHEAR STRAIN ENERGY

The total shear strain energy for a beam is given by the expression

$$U_S = \int_0^L \frac{V^2 dx}{2AG}. \quad (\text{A-10})$$

<sup>1</sup>Underlined numbers in parentheses refer to items in the list of references preceding this appendix.

For the same beam as above and the interval  $0 < x < a$  (where  $x$  is measured from the fixed end),

$$V = \frac{wL}{2} - wx - P. \quad (\text{A-11})$$

For the interval  $0 < x < (L/2) - a$  (where  $x$  is measured from midspan),

$$V = wx \quad (\text{A-12})$$

Substituting  $\eta = \frac{P}{wL/2}$  and  $\alpha = a/L$  in

equations A-11 and A-12

yields

$$V = \frac{wL^2}{2} \left( \frac{1}{L} - 2 \frac{x}{L^2} - \frac{\eta}{L} \right) \quad (\text{A-13})$$

and

$$V = \frac{wL^2}{2} \cdot 2 \frac{x}{L^2} \quad (\text{A-14})$$

These equations when manipulated according to equation A-10 lead to

$$U_S = \frac{w^2 L^5}{8AG} \cdot \alpha \left( 1 - 2\alpha - 2\eta + \frac{4}{3} \alpha^2 + 2\eta\alpha + \eta^2 \right). \quad (\text{A-15})$$

Contours of equation A-15 appear in figure 8. The "valley" in figure 8,  $\partial U_S / \partial \eta = 0$ , has the equation

$$\eta = 1 - \alpha. \quad (\text{A-16})$$

## APPENDIX B.--ZERO NET DISPLACEMENT

The total vertical displacement due to gravity at any location along a beam where both bending and shear deformations are present can be expressed as

$$\delta_{TG} = \delta_{BG} + \delta_{SG}. \quad (B-1)$$

Similarly, the total vertical displacement due to uplift from the truss is

$$\delta_{TT} = \delta_{BT} + \delta_{ST}. \quad (B-2)$$

The practical upper limit of the uplift force occurs when  $\delta_{TG} = \delta_{TT}$  or

$$\delta_{BG} + \delta_{SG} = \delta_{BT} + \delta_{ST}. \quad (B-3)$$

However, the ratio of the bending deflection due to gravity and truss can be expressed as

$$\frac{\delta_{BT}}{\delta_{BG}} = \frac{\eta}{\eta_{Bmax}} \leq 1.0, \quad (B-4)$$

where  $\eta_{Bmax}$  is defined in equation A-9. For shear, the deflection ratio is

$$\frac{\delta_{ST}}{\delta_{SG}} = \frac{\eta}{\eta_{Smax}}, \quad (B-5)$$

where  $\eta_{Smax}$  is defined in equation A-16. Note that there is no requirement that equation B-5 be less than or equal to 1.0 because  $\eta_{Smax}$  is always less than  $\eta_{Bmax}$ . Solving equations B-4 and B-5 for  $\delta_{BT}$  and  $\delta_{ST}$ , respectively, and substituting into equation B-3 yields

$$\delta_{BG} + \delta_{SG} = \frac{\delta_{BG}\eta}{\eta_{Bmax}} + \frac{\delta_{SG}\eta}{\eta_{Smax}}. \quad (B-6)$$

Dividing both sides of equation B-6 by  $\delta_{BG}$  and solving for  $\eta$  leads to

$$\eta_{max} = \frac{1 + \frac{\delta_{SG}}{\delta_{BG}} \eta_{Bmax} \cdot \eta_{Smax}}{\eta_{Smax} + \frac{\delta_{SG}}{\delta_{BG}} \eta_{Bmax}}, \quad (B-7)$$

where  $\eta_{max}$  corresponds to the maximum practical uplift.

From beam theory  $\delta_{BG}$  for a beam fixed at both ends is

$$\delta_{BG} = \frac{wL^2}{24EI} (L^2 - 2aL + a^2) = \frac{wL^2}{2} \cdot \frac{\alpha^2 L^2}{12EI} (1 - \alpha)^2. \quad (B-8)$$

For the same beam,

$$\begin{aligned} \delta_{SG} &= \frac{wL^2}{AG} \frac{a}{2L} - \frac{a^2}{2L^2} \\ &= \frac{wL^2}{2} \frac{\alpha}{AG} (1 - \alpha). \end{aligned} \quad (B-9)$$

Dividing equation B-9 by equation B-8 yields

$$\begin{aligned} \frac{\delta_{SG}}{\delta_{BG}} &= \frac{\frac{1}{AG}}{\frac{\alpha L^2}{12EI} (1 - \alpha)} \\ &= \frac{12EI}{AG} \frac{1}{\alpha L^2 (1 - \alpha)}. \end{aligned} \quad (B-10)$$

For rectangular beams of depth  $h$  composed of a homogeneous, isotropic material having a Poisson's ratio, say, of 0.25, the ratio

$$\frac{EI}{AG} = \frac{2.5}{12} h^2,$$

so that equation B-10 becomes

$$\frac{\delta_{SG}}{\delta_{BG}} = 2.5 \frac{h^2}{L^2} \frac{1}{\alpha (1 - \alpha)}. \quad (B-11)$$

If the shear modulus is effectively only one-tenth what one would expect for a homogeneous isotropic material, the deflection ratio in equation B-11 is 10 times greater.

Since  $\eta_{Bmax}$  and  $\eta_{Smax}$  are also functions of  $\alpha$ , the substitution of equation B-11 into equation B-7 leads to an elaborate expression for  $\eta_{max}$  that is a function of  $\alpha$  and the depth-span ratio  $h/L$ . Equation B-7 has been plotted in figure 10 for two different depth-span ratios and two different shear moduli.

APPENDIX C.--THE EFFECT OF AXIAL LOAD ON BEAM BEHAVIOR

A. Bending deformations only in a beam column

Consider a beam fixed at both ends, subjected to a transverse loading  $w$  and an axial loading  $Q$  (fig. C-1). The internal moment  $M$  required for equilibrium of a beam segment  $x$  long, as measured from the left end is

$$M = \frac{wLx}{2} + Qy - M_0 - \frac{wx^2}{2} \quad (C-1)$$

where  $y$  is the deflection at  $x$  and  $M_0$  is the moment at the left end. If  $y$  downward is taken as positive, the moment-curvature relation is

$$\frac{d^2y}{dx^2} = - \frac{M}{EI} \quad (C-2)$$

Substituting equation C-2 into equation C-1 and separating variables leads to the differential equation

$$\frac{d^2y}{dx^2} + \frac{Qy}{EI} = \frac{1}{EI} - \frac{wLx}{2} + M_0 + \frac{wx^2}{2}, \quad (C-3)$$

for which the solution is

$$y = A \sin kx + B \cos kx + \frac{w}{2Q} x^2 - \frac{wL}{2Q} x + \frac{M_0}{Q} - \frac{wEI}{Q^2}, \quad (C-4)$$

where  $k = \sqrt{Q/EI}$ . Using the condition  $y = dy/dx = 0$  at  $x = 0$  and  $dy/dx = 0$  at  $x = L/2$  in equation C-4, the deflection at the center is

$$y \Big|_{x=L/2} = \frac{wL^2}{Q} \left[ \frac{1}{2kL} \sin \frac{kL}{2} + \frac{1}{2kL} \cot \frac{kL}{2} \cos \frac{kL}{2} - \frac{1}{8} - \frac{1}{2kL} \cot \frac{kL}{2} \right] \quad (C-5)$$

The amplification of the centerspan deflection due to the effect of the axial load can be found from the ratio of that deflection with axial load to the same deflection without axial load.

That is,

$$A.F. = \frac{y \text{ w/axial}}{y \text{ w/o axial}} = \frac{\frac{wL^2}{Q}}{\frac{wL^4}{384EI}} \cdot [ \quad ], \quad (C-6)$$

where the quantity within the brackets is taken from equation C-5. The quantity outside the brackets reduces to

$$\frac{384}{(kL)^2}$$

Equation C-6 can be approximated by the expression

$$A.F. = \frac{1}{1 - \frac{Q}{Q_e}} \quad (C-7)$$

where

$$Q_e = 4\pi^2 EI/L^2 \quad (C-8)$$

the Euler buckling load for the beam. A comparison between equations C-6 and C-7 is given in table C-1 for several values of  $Q/Q_e$ .

B. The buckling load for a column with large shear deformations

Consider now the buckled shape of a beam without lateral load but subjected to an axial load  $Q_c$  sufficient to cause buckling (fig. C-2). The internal moment required for a segment of length  $x$  is

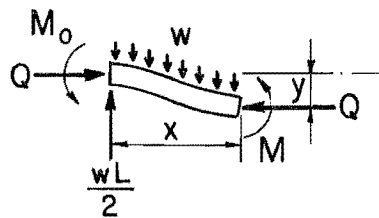
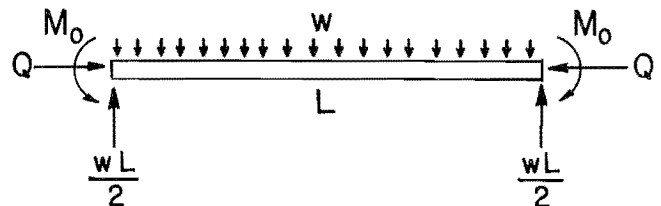


FIGURE C-1.--Fixed-end beam column relations.

TABLE C-1. - Comparison of amplification factors from equations C-6 and C-7

Q/Q <sub>e</sub>	"Exact" equation C-6	Approximate equation C-7
0.01.....	1.010	1.010
.02.....	1.020	1.020
.05.....	1.052	1.053
.10.....	1.110	1.111
.20.....	1.247	1.250
.30.....	1.423	1.429
.40.....	1.658	1.667
.50.....	1.986	2.000

$$M = Q_c y_T - M_o, \quad (C-9)$$

where the total deflection at location x, y<sub>T</sub> = y<sub>B</sub> + y<sub>S</sub> is the sum of the two types of deflections.

As before, the moment-curvature relation is

$$\frac{d^2 y_B}{dx^2} = \frac{M}{EI}, \quad (C-10)$$

In addition there is a moment-slope relation for shear deformation

$$AG \frac{dy_S}{dx} = \frac{dM}{dx}. \quad (C-11)$$

Another moment-slope relation can be found from the first derivative of equation C-9, namely

$$\frac{dM}{dx} = Q_c \frac{dy_T}{dx}. \quad (C-12)$$

Combining equations C-11 and C-12 yields

$$AG \frac{dy_S}{dy} = Q_c \frac{dy_T}{dx}. \quad (C-13)$$

Taking another derivative of equation C-13 gives

$$AG \frac{d^2 y_S}{dx^2} = Q_c \frac{d^2 y_T}{dx^2}. \quad (C-14)$$

Substituting equations C-10 and C-14 into equation C-9 leads to

$$\left(1 - \frac{Q_c}{AG}\right) \frac{d^2 y_T}{dx^2} + \frac{Q_c y_T}{EI} = \frac{M_o}{EI}$$

or, dropping the subscript T,

$$\frac{d^2 y}{dx^2} + k^2 y = \frac{M_o}{\left(1 - \frac{Q_c}{AG}\right) EI}, \quad (C-15)$$

where now

$$k^2 = \frac{Q_c}{\left(1 - \frac{Q_c}{AG}\right) EI}. \quad (C-16)$$

The solution to equation C-15 is

$$y = B \sin kx + C \cos kx + \frac{M_o}{Q_c}, \quad (C-17)$$

for which the constants B and C can be found from the conditions y = dy/dx = 0 at x = 0. Using the condition that y = 0 at x = L leads to

$$y \Big|_{x=L} = \frac{M_o}{Q_c} (1 - \cos kL) = 0. \quad (C-18)$$

Since neither M<sub>o</sub> is zero nor Q<sub>c</sub> is infinite, it follows that

$$\cos kL = 1. \quad (C-19)$$

The smallest non-zero value of kL that satisfies equation C-19 is kL = 2π or, using equations C-8 and C-16,

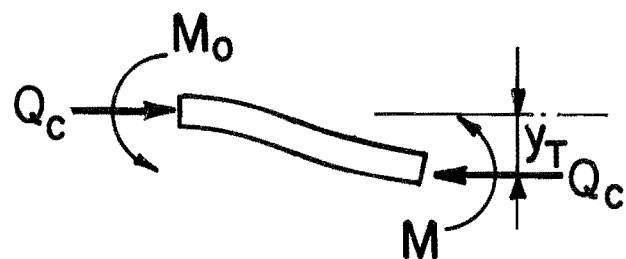


FIGURE C-2.—Fixed-end column relations.

$$k^2 EI = \frac{Q_c}{1 - \frac{Q_c}{AG}} = \frac{4\pi^2 EI}{L^2} = Q_e. \quad (C-20)$$

Solving equation C-20 for  $Q_c$  results in

$$Q_c = \frac{Q_e}{1 + \frac{Q_e}{AG}}. \quad (C-21)$$

Only if  $AG$  is small compared with  $EI$  does equation C-21 yield values of  $Q_c$  significantly different from  $Q_e$ .

### C. Bending and shear deformations combined in a beam column

When both bending and shear deformations occur, equation C-1 can be written as

$$M = \frac{wLx}{2} + Qy_T - M_o - \frac{wx^2}{2}. \quad (C-22)$$

Equation C-10 can be written as

$$\frac{d^2 y_B}{dx^2} = -\frac{1}{EI} \left( \frac{wLx}{2} + Qy_T - M_o - \frac{wx^2}{2} \right). \quad (C-23)$$

Equation C-11 becomes

$$AG \frac{dy_S}{dx} = \frac{dM}{dx} = Q \frac{dy_T}{dx} + \frac{wL}{2} - wx,$$

which when another derivative is taken becomes

$$\frac{d^2 y_S}{dx^2} = \frac{1}{AG} \left( Q \frac{d^2 y_T}{dx^2} - w \right). \quad (C-24)$$

Adding together equations C-23 and C-24 and rearranging terms yields

$$\frac{d^2 y}{dx^2} + k^2 y = \frac{1}{1 - \frac{Q}{AG}} \left[ \frac{1}{EI} \left( M_o - \frac{wL}{2} + \frac{wx^2}{2} \right) - \frac{w}{AG} \right], \quad (C-25)$$

where now

$$k^2 = \frac{Q}{1 - \frac{Q}{AE} EI}. \quad (C-26)$$

Using the same boundary conditions that led to equation C-5, it can be written for any location  $x = a$  along the beam

$$y \Big|_{x=a} = \left[ \frac{wLAG}{2kQ (AG - Q)} \right] \sin ka + \left[ \frac{wLAG \cot \frac{kL}{2}}{2kQ (AG - Q)} \right] (\cos ka - 1) + \frac{wL^2}{2Q} - \frac{wLa}{2Q}. \quad (C-27)$$

The beam deflection in the absence of axial load can be shown to be equal to

$$y \Big|_{x=a} = \frac{wa^2}{24EI} (a^2 + L^2 - 2aL) + \frac{1}{AG} \left( \frac{wLa}{2} - \frac{wa^2}{2} \right). \quad (C-28)$$

Using the substitution  $\alpha = a/L$ , the ratio of equation C-27 to C-28 becomes the amplification factor

$$A.F. = \frac{AG}{Q} \left[ \frac{\sin \alpha kL + (\cos \alpha kL - 1) \cot \frac{kL}{2}}{kL \left( 1 - \frac{Q}{AG} \right)} + \alpha^2 - \alpha \right], \quad (C-29)$$

$$\frac{L^2 AG}{12EI} \alpha^2 (\alpha^2 + 1 - 2\alpha) + \alpha - \alpha^2$$

which can also be approximated by equation C-7 except that  $Q_e$  is replaced by  $Q_c$  or

$$A.F. = \frac{1}{1 - Q/Q_c}. \quad (C-30)$$

In normal elastic behavior of rectangular cross sections, the quantity

$$\frac{AGL^2}{2EI} = \frac{4.6L^2}{h^2} \quad (C-31)$$

if Poisson's ratio is taken as 0.3 and  $h$  is the depth of the beam. To demonstrate the conservative validity of the approximation in equation C-30 in place of equation C-29, table C-2 compares several combinations of parameters.

TABLE C-2. - Comparison of amplification factors from equations C-29 and C-30

Equation	$G/G_{normal}$	$L/h$	Amplification factors at $Q/Q_c$ of--		
			0.01	0.10	0.50
C-29 <sup>1</sup> .....	1.0	20	1.009	1.095	1.840
	1.0	5	1.008	1.088	1.755
	.1	20	1.008	1.089	1.774
	.1	5	1.009	1.009	1.838
C-30.....	NAp	NAp	1.010	1.111	1.998

NAp Not applicable.

<sup>1</sup> $\alpha = 0.2$ .

## APPENDIX D.---ABBREVIATIONS AND SYMBOLS USED IN THIS REPORT

NOTE.---This list does not include the unit of measure abbreviations listed at the front of this report.

a	bearing bracket position measured from the rib.	$\alpha$	dimensionless position parameter $a/L$ .
A	effective cross-sectional area of the roof beam.	$\beta$	dimensionless bolt tension parameter $2T/wL$ .
A.F.	amplification factor	$\delta_{BG}$	bending displacement due to gravity.
E	effective modulus of elasticity of the roof beam.	$\delta_{BT}$	bending displacement due to the truss.
G	effective shear modulus of the roof beam.	$\delta_{SG}$	shear displacement due to gravity
h	depth of the roof beam	$\delta_{ST}$	shear displacement due to the truss.
I	effective moment of inertia of the roof beam.	$\delta_{TG}$	total displacement due to gravity
$l$	length of the angle bolt excluding the anchorage.	$\delta_{TT}$	total displacement due to the truss.
L	width of entry	$\Delta_P$	beam displacement due to bending at the location of the bearing bracket.
M	bending moment in the roof beam	$\eta$	dimensionless uplift parameter $2P/wL$ .
N.G.	no good	$\eta_{Bmax}$	value of $\eta$ from equation A-9
P	uplift force supplied by the truss.	$\eta_{Smax}$	value of $\eta$ from equation A-16
Q	effective horizontal force exerted by in situ stresses.	$\theta$	angle-bolt slope measured from the horizontal.
$Q_c$	horizontal force required to produce beam buckling involving both bending and shear.	$\lambda$	dimensionless bolt length parameter $l/L$ .
$Q_e$	horizontal force required to produce beam buckling due to bending alone.		
T	tension in the angle bolt		
$U_B$	strain energy due to bending		
$U_S$	strain energy due to shear		
V	shear in the roof beam		
w	unit weight of the roof beam material.		